CrossMark

# Secular changes in environmental stresses and eukaryotes during the Early Triassic to the early Middle Triassic

Ryosuke Saito [a,*], Kunio Kaiho [a,*], Masahiro Oba [a], Jinnan Tong [b], Zhong-Qiang Chen [b], Satoshi Takahashi [a], Jing Chen [b], Li Tian [b], Raman Kumar Biswas [a]

[a] Institute of Geology and Paleontology, Tohoku University, Sendai 980-8578, Japan
[b] State Key Laboratory of Biogeology and Environmental Geology, China University of Geosciences, Wuhan 430074, China

## ABSTRACT

The Early Triassic, following the end-Permian mass extinction, was an interval of severe low diversity. Increasing amounts of evidence demonstrate that variable environmental stresses were widespread and intense after the end-Permian mass extinction. Here we report biomarkers from lowest Triassic to lower Middle Triassic strata in South China (Qingyan and Chaohu sections), including biomarkers for environmental stress (2-methyl hopane index) and eukaryotic algae (steranes and $C_{21}$ $n$-alkylbenzene ratio). Using the 2-methyl hopane index, we detected the persistence of environmental stress during most of the Early Triassic. Using steranes and the $C_{21}$ $n$-alkylbenzene ratio, we found a gradual increase in the biomass of eukaryotic algae during the Early to early Middle Triassic. A decrease in environmental stress in the Qingyan section (Leidapo Member) during the early Middle Triassic was synchronous with the "explosion" of the Qingyan Biota, which is characterized by a high abundance and diversity of invertebrate marine animals. Because the environmental stresses revealed by the 2-methyl hopane index encompass various factors (e.g., pH and temperature), we cannot identify the exact stresses at that time; however, our results reflect the amelioration of harsh environments for life during the interval of complete biotic recovery.

© 2016 Elsevier B.V. All rights reserved.

## 1. Introduction

The end-Permian mass extinction at 252.17 Ma (Shen et al., 2011) was the greatest known mass-extinction event on Earth. The Early Triassic, immediately following the event, has been the primary focus of studies of the interactions between environmental stresses and biota. A number of studies have reported hostile conditions for life during the Early Triassic, including global warming (Joachimski et al., 2012; Sun et al., 2012), massive terrigenous detrital input stress caused by enhanced soil erosion (Algeo and Twitchett, 2010; Zhao et al., 2012), oceanic anoxia (e.g., Wignall and Hallam, 1992; Isozaki, 1997; Tian et al., 2014a), unstable carbon–sulfur cycles (Song et al., 2014), loading of toxic metals (Grasby et al., 2015), hypercapnia (Knoll et al., 1996; Tian et al., 2014b), oceanic acidification (Clapham et al., 2013), worldwide depletion of stratospheric ozone (Kump et al., 2005), and unusual oceanic chemistry (Abdolmaleki and Tavakoli, 2016).

These deleterious conditions for life probably suppressed the full biotic recovery from the end-Permian mass extinction and were similar to conditions during the Precambrian. The sedimentary response to these conditions was remarkable during the Early Triassic, as the Lower Triassic sedimentary record is characterized by low bioturbation, microbialites, giant ooids, sea-floor fan precipitates, and wrinkle structures, all of which are characteristic of the Precambrian–Cambrian ocean (Schubert and Bottjer, 1992; Woods et al., 1999; Pruss and Bottjer, 2004; Pruss et al., 2005; Knoll et al., 2007; Chen et al., 2011, 2014; Chen and Benton, 2012; Li et al., 2013, 2015; Tian et al., 2015a, 2015b). These sedimentary responses indicate that during the Early Triassic the ocean conditions returned to those of the Precambrian.

Paleoenvironmental stresses (e.g., temperature, pH, and osmotic stress) can be measured by lipid biomarker analysis. The 2-methyl hopane index (2-MHI), which has been a widely used cyanobacterial proxy based on biomarkers (Summons et al., 1999; Xie et al., 2005, 2010; Knoll et al., 2007; Cao et al., 2009), has recently been updated by molecular biological studies (Kulkarni et al., 2013; Ricci et al., 2014, 2015; Wu et al., 2015). The revised 2-MHI index is a proxy of paleoenvironmental stress (Kulkarni et al., 2013; Ricci et al., 2014, 2015; Wu et al., 2015). It has been inferred that the Precambrian ocean was a stressful environment for life because the 2-MHI values for this time interval (>10) are higher than those for the Phanerozoic, except for certain intervals (Knoll et al., 2007).

For eukaryotic algae, the Early Triassic was also a time of lowest diversity. Falkowski et al. (2004) suggested that the transition from green algal to red algal lineages occurred during the Early Triassic, probably triggered by the end-Permian mass extinction. In addition, an algal

gap at the beginning of the Early Triassic (Sun et al., 2012) indicates that cyanobacteria were the dominant primary producers in Early Triassic seas. However, the distribution of eukaryotic algae during the Early Triassic has yet to be investigated in detail.

To reconstruct the history of environmental stresses and eukaryotic algae during the Early to early Middle Triassic, we collected samples from the Chaohu and Qingyan sections in South China (Fig. 1) for lipid biomarker analysis.

## 2. Geological and stratigraphical settings

Two South China sections (Chaohu and Qingyan) were examined (Fig. 1). The Lower Triassic successions exposed in the North Pindingshan, West Pindingshan, and South Majiashan sections of the Chaohu area (Anhui Province, southern China) were sampled. During the Early Triassic, southern China was located in the low-latitude eastern Paleotethys Ocean. The Early Triassic depositional environments recorded in Chaohu varied from distal offshore ramp to shore face, to marginal seas (Chen et al., 2011). High-resolution correlation of conodont zones from the Lower Triassic units (Tong et al., 2003) made it possible to integrate the successions into a composite lithologic section. Lithologically, the Lower Triassic sequence is characterized by the mudstone-dominated successions of the Yinkeng Formation in the lower part and the limestone-dominated successions of the Nanlinghu Formation in the upper part. The alternating thinly bedded mudstones and muddy limestone (marlstones) units between these two formations are referred to collectively as the Helongshan Formation. In general, the mudstone content decreases and the carbonate content increases up through the section. In Chaohu, both conodonts and ammonoids were abundant throughout the entire Lower Triassic (Tong et al., 2003, 2004; Zhao et al., 2008). Based on a regional correlation, the Early–Middle Triassic boundary was placed at the base of the Dongmaanshan Formation in the area (Li and Ding, 1981), although typical Anisian fossils have not been recovered from Chaohu.

During the Early and Middle Triassic the Qingyan area of Guiyang city, Guizhou Province was situated on a carbonate ramp, at the junction between the Yangtze platform in the north and west, and the relatively deep Nanpanjiang Basin in the south and east (Chen et al., 2010a). In the Qingyan section, the lowest Triassic strata are assigned to the Shabaowan Formation. They consist of calcareous mudstone and thinly bedded limestone containing the bivalve *Claraia* spp. and the ammonoid *Ophiceras* spp. (Chen et al., 2010a, c), both of which are characteristic of the Griesbachian assemblages in South China. Overlying the Shabaowan Formation, the Luolou Formation consists of thinly bedded muddy limestone with abundant bivalve and ammonoid fossils (Chen et al., 2010a, c). The upper part of the Lower Triassic is referred to as the Anshun Formation, comprised of thinly bedded dolomitic

limestones, vermicular limestone, and dolomite (Chen et al., 2010a, c). The early Middle Triassic strata belong to the Qingyan Formation, which is composed, in ascending order, of the Xiaoshan, Mafengpo, Yingshangpo, Leidapo, and Yuqing Members (Chen et al., 2010a). The Xiaoshan Member is characterized by alternating carbonate breccia, limestone, and calcareous shale. The Mafengpo Member is dominated by calcareous shale with minor interbeds of breccia and thinly bedded limestone. The Yingshangpo Member is characterized by gray, medium-bedded limestone. The upper part of the Leidapo Member is composed of alternating calcareous mudstone and muddy limestone. The Yuqing Member consists mainly of muddy limestone and dolomitic limestone. Dating of the Qingyan deposits is based on conodont and ammonoid zones (Chen et al., 2010a, b, c).

## 3. Methods

Two hundred and eighty three carbonate, shale, and marl samples were collected from the Chaohu, and Qingyan sections for organic geochemical assessment (Fig. 1). Approximately 20–100 g of each sample was powdered following removal of any apparent surface contamination. The powdered samples were extracted for 48 h using a Soxhlet apparatus and a dichloromethane:methanol mixture (7.5:1 $v/v$). The extracts were dried over $Na_2SO_4$ and concentrated by evaporation under reduced pressure. The concentrated extracts were separated by elution into nine fractions (F) on a silica gel column (0.6 g of silica, 63–200 μm mesh) using the following solvents (Oba et al., 2006): 2 ml of $n$-hexane (F1a); 4 ml of $n$-hexane (F1b); 3 ml of $n$-hexane/toluene 3:1 $v/v$ (F2); 3 ml of $n$-hexane/ethyl acetate 19:1 $v/v$ (F3); 3 ml of $n$-hexane/ethyl acetate 9:1 $v/v$ (F4); 3 ml of $n$-hexane/ethyl acetate 17:3 $v/v$ (F5); 3 ml of $n$-hexane/ethyl acetate 4:1 $v/v$ (F6); 3 ml of $n$-hexane/ethyl acetate 3:1 $v/v$ (F7); and 10 ml of methanol (F8). Aliphatic hydrocarbon fractions (F1a) and aromatic hydrocarbon fractions (combinations of F1b and F2) from each extract were analyzed by gas chromatography–mass spectrometry.

The organic compounds were identified using an Agilent 6893 gas chromatograph interfaced to an Agilent 5973 mass-selective detector (MSD) operated with an ionizing-electron energy of 70 eV and scanned from $m/z$ 50 to 550 with a scan time of 0.34 s. A fused silica HP-5MS capillary column (30 m, 0.25 mm internal diameter, 0.25 μm film thickness) was used, with helium as the carrier gas. Samples were injected at 50 °C and held at that temperature for 1.0 min. The temperature was then raised to 120 °C at a rate of 30 °C/min, then to 310 °C at a rate of 5 °C/min, and finally held constant for 20 min. Multiple reaction monitoring (MRM) analyses for saturated hydrocarbons were performed using an Agilent 7890B GC equipped with an Agilent 7000 triple quadrupole mass spectrometer and HP-5MS capillary column (30 m, 0.25 mm internal diameter, 0.25 μm film thickness), using helium and nitrogen as the carrier gas and the collision gas, respectively. Samples were injected at 50 °C and held at that temperature for 1.0 min. The temperature was then raised to 250 °C at a rate of 30 °C/min, then to 310 °C at a rate of 5 °C/min, and finally held constant for 20 min. Biomarkers such as $C_{27-35}$ hopanes, gammacerane, $C_{32}$ 2α-methylhopanes, $C_{19}$ tricyclic terpane and $C_{23}$ tricyclic terpane, $C_{27-30}$ steranes, $C_{20-22}$ $n$-alkylbenzenes were identified based on published retention times and mass spectral peaks (e.g., Summons and Jahnke, 1990; Peters et al., 2005; Ivanova and Kashirtsev, 2010). Peak areas of hopanes, gammacerans, and steranes were obtained by each transition of MRM. Peak areas of $C_{20-22}$ $n$-alkylbenzenes were obtained by $m/z$ 92.

## 4. Results and discussion

We used multiple biomarkers including $C_{27-35}$ hopanes as bacterial proxies, gammacerane for a redox proxy, and steranes and $n$-alkylcyclobenzene as eukaryotic algae proxies (Figs. 2–4).
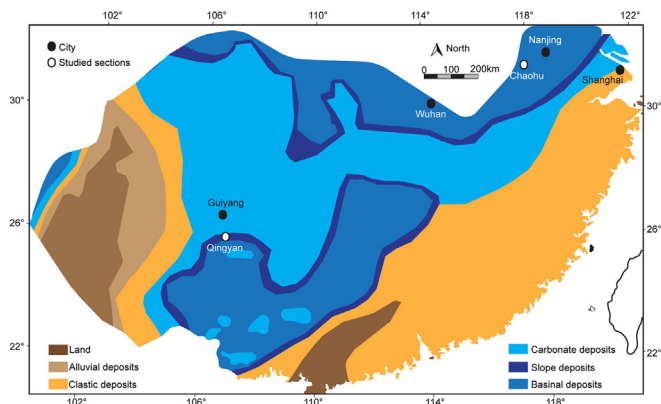


**Fig. 1.** The Chaohu, and Qingyan sections (base map after Song et al., 2013).